



## Journal of Advanced Research in Applied Mechanics

Journal homepage:  
[https://semarakilmu.com.my/journals/index.php/appl\\_mech/index](https://semarakilmu.com.my/journals/index.php/appl_mech/index)  
ISSN: 2289-7895



# Effect of Torsional Load on Electrical and Mechanical Properties/Behaviour of Stretchable GNP-Ag Conductive Ink

Ismaniza Ismail<sup>1,2</sup>, Mohd Azli Salim<sup>2,\*</sup>, Nor Azmmi Masripan<sup>2</sup>, Adzni Md. Saad<sup>2</sup>, Mohd Zaid Akop<sup>2</sup>, Chew Kit Wayne<sup>3</sup>, Chonlatee Photong<sup>4</sup>

<sup>1</sup> Jabatan Kejuruteraan Mekanikal, Politeknik Ungku Omar, Ipoh, Perak, Malaysia

<sup>2</sup> Fakulti Teknologi dan Kejuruteraan Mekanikal, Universiti Teknikal Malaysia Melaka, Melaka, Malaysia

<sup>3</sup> School of Chemistry, Chemical Engineering and Biotechnology, Nanyang Technological University, Singapore

<sup>4</sup> Faculty of Engineering, Maharakham University, Thailand

### ARTICLE INFO

#### Article history:

Received 30 January 2024

Received in revised form 17 March 2024

Accepted 31 March 2024

Available online 30 May 2024

#### Keywords:

Stretchable conductive ink; graphene nanoplatelet; silver flakes; resistivity

### ABSTRACT

Stretchable conductive inks (SCIs) have gained significant attention in recent years due to their potential applications in flexible and wearable electronics. Graphene nanoplatelet (GNP) hybridization conductive ink is a promising material for stretchable electronics due to its high electrical conductivity and excellent mechanical properties. However, the resistivity of GNP ink on flexible substrates can be affected by various factors, such as the torsion of the substrate. This paper aims to investigate the effect of torsional load in terms of the electrical and mechanical behaviour of hybridization conductive ink between GNP and Ag. The research was carried out on the formulation and performance of GNP hybrids using GNP and silver flakes (Ag). The GNP hybrid ink was printed on a copper substrate using a mesh stencil method and cured at 250 °C for an hour. The resistivity was evaluated at room temperature before and after the torsional tests in terms of electrical characteristics. The finding exposed that the resistivity values for each of the three samples of torsional tests significantly changed after 1000 cycles. Eventually, the resistance value at cycle 5000 rose due to the damaging impact of increasing the number of torsional cycles on the sample. In future work, it is recommended that the evaluation is made under temperature dependence and supported by SEM images.

## 1. Introduction

Stretchable conductive inks (SCIs) have emerged as a promising material for flexible and wearable electronics due to their ability to maintain their electrical conductivity under mechanical strain. The development of stretchable and flexible devices has enabled novel interaction mechanisms for applications such as wearable electronics, consumer electronics, electronic skin (E-skin), robotics, etc. [1]. The inks are composed of conductive materials that can maintain their electrical conductivity under mechanical strain, making them suitable for use in applications where conventional rigid

\* Corresponding author.

E-mail address: [azli@utem.edu.my](mailto:azli@utem.edu.my)

<https://doi.org/10.37934/aram.117.1.2234>

electronic devices are unsuitable. According to [2], the development of stretchable electronics is highly dependent on the performance of the interconnected components, which must be able to retain their electrical conductivity while being exposed to extreme deformation. Specifically, the stretchable interconnection is essential for the fabrication of antennas and sensors for wearable electronics. Several conducting additives, such as carbon- and noble metal-based nanomaterials, have been incorporated into elastomeric matrices to create nanocomposites with the desired conductivity and stretchability [3].

Conductive inks are used to produce electrical conductors on printed items. The use of conductive inks has become a fresh and innovative method to advance electronics manufacturing processes. Due to their function in connecting the various components of the devices, conductive inks are regarded as crucial for the fabrication of all stretchable, flexible, and wearable electronic applications [4]. Numerous types of conductive inks, such as metal-based (silver, gold, and copper) materials, conducting polymers, and other conductive organic materials, such as carbon-based inks (graphene, graphene oxide, and carbon nanotube), have been used for a variety of printed, flexible, and wearable electronic applications [5-8]. The basic electrical, physical and mechanical properties of GNP are  $10^6$  S/m, 130 GPa and 1 TPa. For Ag, there are  $6.3 \times 10^7$  S/m, 170 MPa and 83 GPa.

Recently, graphene materials consisting of a single layer or more layers of graphene flakes have attracted a great deal of interest as excellent conductive fillers due to their optical transparency, high conductivity, flexibility, and comparatively low cost compared to their metallic and polymer counterparts. As a result, conductive inks based on graphene have been frequently reported [9] notably as conductive ink for flexible and elastic printed electronics. Design and production of graphene hybrid complexes to improve their conductivity have been the subject of intensive study. By mixing the combined graphene with conductive polymer or metal particles, hybrid inks may optimize the qualities of the two materials by combining them for diverse applications [10]. According to [11], previous research has primarily focused on hybrid graphene and metal-based composite materials to enhance the conductivity of pure graphene inks. Silver nanoparticles (AgNP) conductive ink is the most popular nanoparticle-based conductive ink for use in printed electronics due to its superior oxidation resistance, electrical conductivity, and other desirable physical properties that provide extraordinary substrate adhesion.

The electrical conductivity and resistance of the ink under bending, twisting, or stretching are important factors that determine its performance and reliability. In a study by [12], Ag inkjet printing on PI substrates was examined at torsion angles of up to 40 degrees. The distance between the extremities of the bent microstrip line varied between 5cm and 9.2cm. Additionally, torsion angles (0–40°) were used to distort the microstrip lines. The radio frequency (RF) performance and characteristics (transmission and return losses) nearly remained unchanged. Another study by [13] investigated the wearable thermistor ECG sensor affixed on PI subjected to deformation and torsion tests. 1,000 cycles of bending with radii of 10 mm and 5 mm, followed by 1,000 cycles of twisting (30°), did not affect the electrical resistance. Besides that, [14] aerosol-jet additively printed and thermally sintered (at various temperatures) commonly used trace geometries on flexible PI substrates intended for wearable applications. Twisting and bending were performed. In realtime, the resistances of the traces were measured and recorded. According to the data, conductive traces printed with silver nanoparticles have a reduced susceptibility to failure at 250 C and under shear load. Cyclic deformation and twisting provide additional proof of the same. In comparison to other geometries, zigzag traces tend to fail more frequently. In addition, researchers [15] examined the effects of monotonic and cyclic loading on flexible electronics. On both PI and PET substrates, devices with screen-printed silver conductors were analysed. Over 5000 cycles, cyclic twisting to 135° or shear strains of  $2.99 \times 10^{-3}$  induced negligible resistance changes (less than 1.5%).

The purpose of this study is to investigate the effect of torsional load in terms of the electrical and mechanical behaviour of hybridization conductive ink between GNP and Ag. By characterizing the resistivity of the ink as a function of the torsional test, insights can be gained into the electrical performance and mechanical reliability of the material. The results of this study provide valuable information for the development of flexible and stretchable electronic devices based on GNP hybridization conductive ink.

## 2. Methodology

In this research, a GNP hybrid conductive ink consisting of several conductive fillers was developed. The GNP hybrid formulation composed of GNP, Ag, and SA as conductive materials was synthesized with the organic solvents of ethanol, butanol, and terpineol. The sample preparation procedure for the hybrid GNP includes ink formulation, mixing process for powder and paste, ink printing, curing, and characterization of the samples.

### 2.1 Formulation of GNP Hybrid

The formulation of GNP hybrid used a specified percentage of filler loading and solvent, according to Table 1 below. The GNP hybrid formulation was based on the approach described by [15] for developing hybrid conductive ink. The powder or liquid substance to be weighed should be placed in a clean beaker and weighed using a digital scale.

**Table 1**

Composition of GNP hybrid conductive ink

Sample	GNP (g)	Ethanol (ml)	Silver flake, Ag (g)	Silver acetate, SA (g)	Ratio Butanol: Terpineol (drop)
1 set	0.05	5	0.4292	0.042	3:3

### 2.2 Mixing Process

The mixing process of GNP hybrid is divided into two parts, which are powder and paste. Basically, the mixing process involved combining various composition to create the homogeneous mixture that can be used as a conductive ink for printing the sample. Based on the formulation, the procedure was prepared for 10 sets, respectively. The 0.5 g of GNP was mixed with 50 ml ethanol in a small beaker. The beaker was covered with aluminum foil to prevent the ethanol from drying rapidly throughout the experiment. These two materials were combined using an ultrasonic bath for 10 minutes. The sonication method using an ultrasonic bath was used as the primary fabrication method during the whole experiment. The 4.292 g silver flakes, Ag were added to the GNP/ethanol mixture and continued sonication for 1 hour. Throughout the sonication procedure, the dispensability of GNP in ethanol and Ag was observed. Figure 1 illustrates the sonication process using an ultrasonic bath.

The mixture was then added with 0.42 g of silver acetate, SA, and sonicated for an hour. Next, the solution was heated at 70 °C on a hotplate with 200 rpm of stirring until the balance of the ethanol evaporated. After the stirring process, the mixture was transferred to a small white porcelain beaker and cured in an oven at 250 °C for 1 hour. After the curing process, the cold mixture was mashed finely until it produced a powder. The powder was transferred to a container for the preparation of GNP hybrid paste.



**Fig. 1.** The sonication process using an ultrasonic bath

The powder was weighted at 4.68 g in a small container. Then, 45 drops of butanol and 45 drops of terpineol were alternately added to the powder as depicted in Figure 2. The mixture was placed in the Thinky mixer to obtain uniform blending. The ink paste consistency was finally obtained and appropriate for printing.

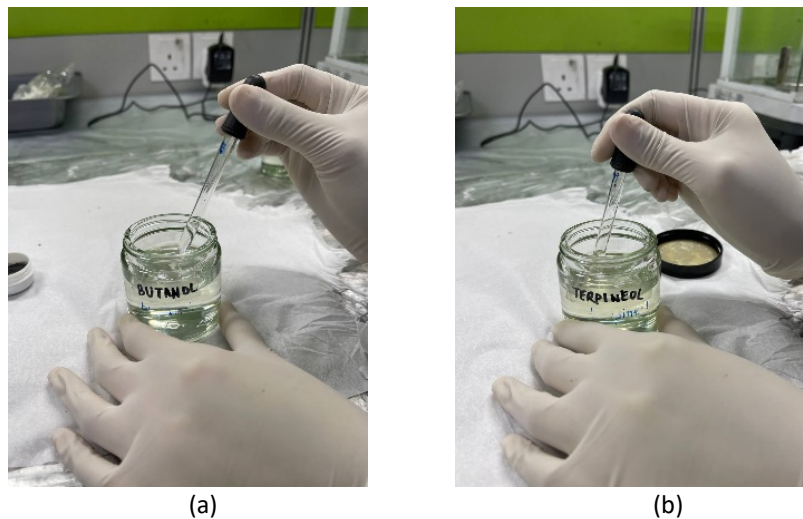


**Fig. 2.** The drops added to the powder (a) butanol (b) terpineol

### 2.3 Printing Process

The GNP hybrid paste was printed on copper substrates using a mesh stencil method. The used mesh stencil has a thickness of 10  $\mu\text{m}$ . The process started by placing the substrate below the mesh stencil, and then the paste was placed on the 3 mm x 3 mm grid. The paste was printed on the three selected points of the substrate strip, using a scraper until it was visible as illustrated in Figure 3. After printing, the mesh stencil was cleaned, and the procedure was repeated for all 9 samples.

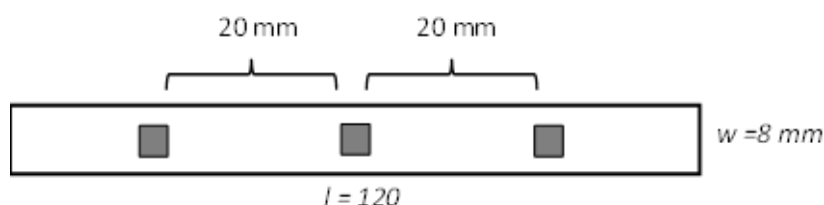


**Fig. 3.** Schematic diagram of printing points

## 2.4 Curing Process

The curing procedure is a post-treatment performed after the printing of conductive ink. This procedure is required to strengthen the binding between the filler and binder particles. Curing is also used to strengthen the bond between the ink and the substrate. In this study, the universal oven UF55 is used for the curing process. After setting up the oven, the printed samples were placed on a tray and cured in the oven at 250 °C for an hour. Then, all the cured samples were fully soaked at room temperature.

## 2.5 Sample Characterization

The characterization for this study focuses on electrical properties. The samples were prepared specifically according to each relevant test standard. The resistance of the material used to form the circuit determines the conductivity of the circuit. Different weight percentages of conductive filler in the formulation provide various resistance levels.

### 2.5.1 Electrical characteristic

The functionality of cured samples was determined by measuring the samples' electrical characteristics by followed the ASTM D2652-22. In this experiment, a multimeter as in was used to measure the resistance of the conductive ink at room temperature. The scale of the multimeter was set at a range of 200  $\Omega$  before being applied to the samples. Each sample consists of three printed inks. The resistance of each ink was tested at three distinct points, as specified in Figure 4 below. The total resistance measurement for each sample is thus nine. Each sample reading will be averaged and monitored for further discussion.

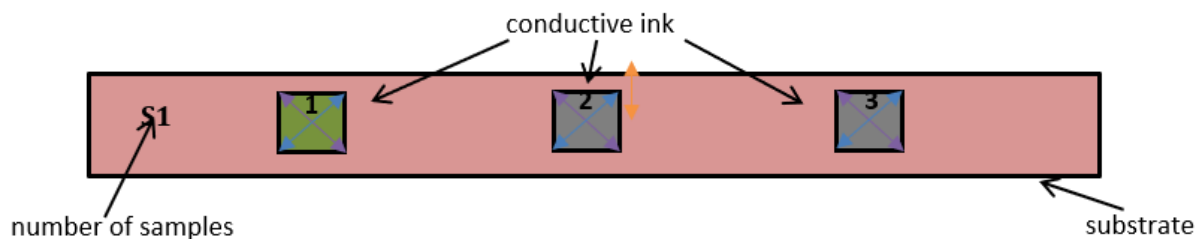


Fig. 4. Schematic diagram of printed ink with testing points

By analysing the data, the volume of resistivity is utilised to assess the level of electrical resistance existing in the circuit and the efficacy of the established conductivity. The selected formulation criteria are based on the suitable volume of resistivity and will be applied realistically across all tested formulations. The resistivity formula is shown in Eq. (1).

$$\rho = RA/l \quad (1)$$

where,  $\rho$  = resistivity ( $\Omega \cdot m$ ),  $R$  = resistance ( $\Omega$ ),  $A$  = cross sectional area ( $m^2$ ) and  $l$  = length of conductor (m).

### 2.5.2 Mechanical characteristic

The reliability of conductive ink was determined by mechanical cyclic tests by followed ASTM A938-18 and ASTM E2207-15. A torsional test was carried out to measure the durability of conductive ink before and after the experiment at room temperature (20.1 °C). The torsion test was used to determine the resistance and resistivity of conductive ink while the process was operating at specific cycles. For each test, the number of cycles is 1000, 3000, and 5000. In this experiment, three samples were selected for respective torsion tests.

For cyclic torsional test, three samples utilized for the torsion test were labeled as S4, S5, and S6 respectively. Figure 5 shows the sample of conductive ink used in the torsional test. The samples were held by two holders, one was fixed and the other was repeatedly rotated to generate the twisting motion in the samples. The twisting deformation was rotated clockwise and anticlockwise alternately during the tests. The twisting angle was  $\pm 90^\circ$ . Figure 6 illustrates the torsion test machine used for this experiment. The resistance measurements for the torsion test were obtained at specific points using a multimeter when the counter reached 1000. This process was repeated with a cycle of 3000 and 5000 as well.



Fig. 5. Samples used for torsional test

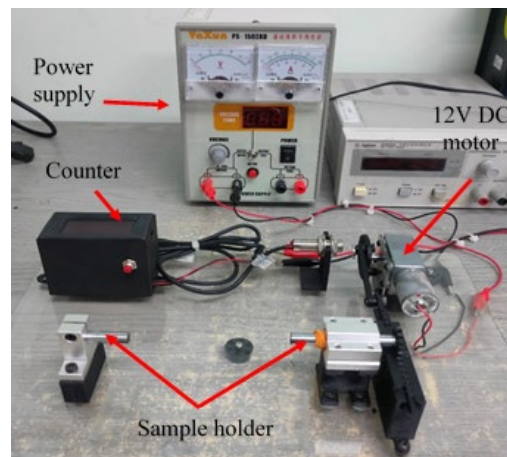


Fig. 6. Torsion test machine

## 3. Results

### 3.1 Resistance and Resistivity of GNP Hybrid at Room Temperature

The experiment was conducted to measure the value of resistance and resistivity of test samples at room temperature (RT). They were measured at three specified points per ink using a multimeter, yielding a total of nine data points per sample thus contributing to the resistance value. Resistivity was calculated using the average results of resistance at each point pattern number. Table 2 shows the resistivity measurement results of average resistance, average resistivity, and standard deviation values for all test samples.

There is no standard benchmark for calculating standard deviation, however, the best standard deviation must have the lowest number. It shows how closely the data is clustered around the mean or average, as well as how far the data is dispersed from the mean or average [16,17]. From Table 2, sample S7 has a very large standard deviation as compared to other samples. It implies that the data is widely dispersed from the mean, indicating that their average resistivity is the greatest. Meanwhile, sample S6 has the smallest standard deviation indicating that the data are gathered close to the mean. This also demonstrates that the ink sample has the lowest and most constant average resistivity.

**Table 2**  
 Measurement of resistivity of test samples

Sample	Average Resistance ( $\Omega$ )	Average Resistivity ( $\Omega.m$ )	Standard deviation ( $\Omega.m$ )
S1	1.293	1.293e-05	8.190e-07
S2	1.089	1.089e-05	6.939e-07
S3	1.063	1.063e-05	3.208e-07
S4	1.070	1.070e-05	1.096e-06
S5	1.089	1.089e-05	1.160e-06
S6	1.059	1.059e-05	2.796e-07
S7	0.963	0.963e-05	1.326 e-06
S8	1.081	1.081e-05	7.143 e-07
S9	1.215	1.215e-05	6.700 e-07

### 3.2 Measurement of Resistance and Resistivity of GNP Hybrid on Torsion Test

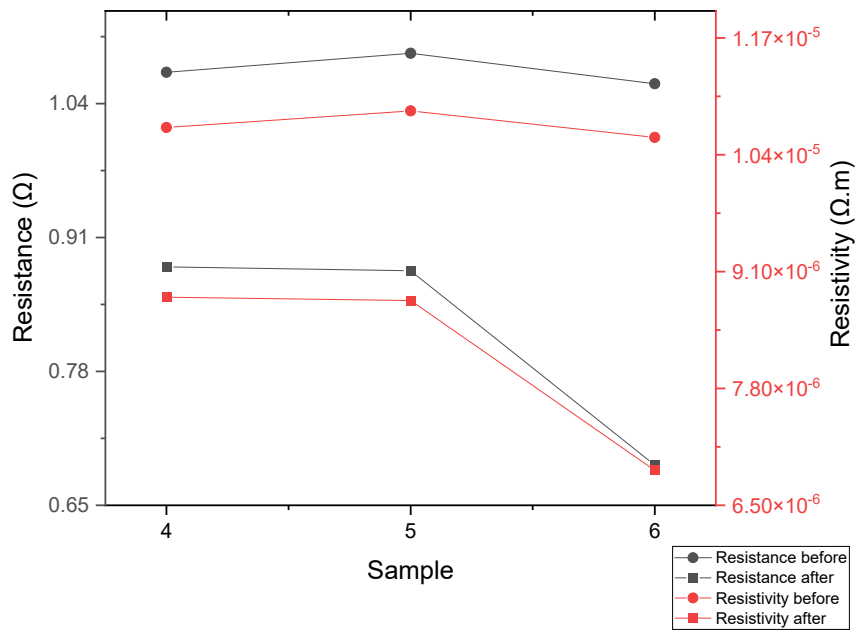
The experiment was carried out to measure the value of resistance and resistivity of test samples on a torsion test at room temperature (RT). This torsion test was performed to assess the resistivity of conductive ink after the twisting procedure had been completed. They were measured at three specified points per ink using a multimeter, yielding a total of nine data points per sample thus contributing to the resistance value. The average results of resistance at each point pattern number are used to calculate resistivity.

Table 3 shows the resistivity measurement data as the average resistance and average resistivity of three samples for 1000 cycles of torsional testing. The average resistance for S4, S5, and S6 samples is lower than before testing.

**Table 3**  
 Measurement of resistivity of the test samples for 1000 cycles of torsional testing

Sample	Average Resistance ( $\Omega$ )		Average Resistivity ( $\Omega.m$ )	
	before	after	before	after
S4	1.070	0.881	1.070e-05	8.815e-06
S5	1.089	0.878	1.089e-05	8.778e-06
S6	1.059	0.689	1.059e-05	6.889e-06
Average	1.073	0.816	1.073e-05	8.160e-06

Figure 7 depicts the average resistance, including the average resistivity of all samples S4, S5, and S6 after 1000 cycles of torsion testing. According to [18], greater strain was produced near the edge and under situations of considerable torsional angle. Consequently, this causes a decrease in the resistivity value due to possible damage to the samples.



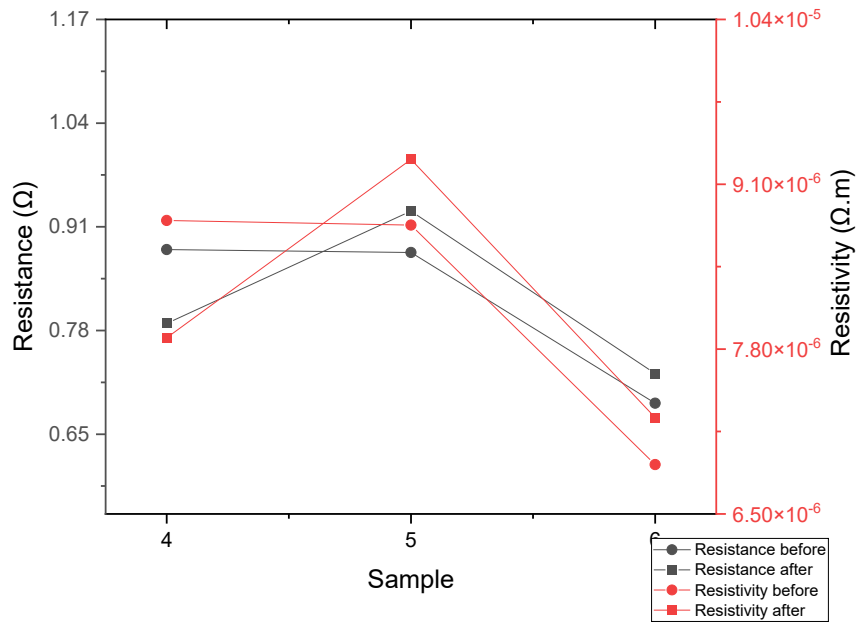
**Fig. 7.** Resistance and resistivity before and after torsion test on test samples for 1000 cycles

Table 4 shows the resistivity measurement data as average resistance and average resistivity of samples S4, S5, and S6 for 3000 cycles of torsional testing. Before bending tests, the average resistances for S4 are slightly higher than the average resistances after tests. Meanwhile, the average resistance and resistivity for samples S5 and S6 appeared to increase. The resistance on the sample can be unstable and too high as compared to others due to the minimal graphene in the filler loading [18].

**Table 4**  
 Measurement of resistivity of the test samples for 3000 cycles of torsional testing

Sample	Average Resistance (Ω)		Average Resistivity (Ω.m)	
	before	after	before	after
S4	0.881	0.789	8.815e-06	7.889e-06
S5	0.878	0.930	8.778e-06	9.296e-06
S6	0.689	0.726	6.889e-06	7.259e-06
Average	0.816	0.815	8.160e-06	8.148e-06

Figure 8 illustrates a high level of average resistance, as well as average resistivity, for samples S5 and S6 after 3000 cycles of torsion testing. However, the resistivity average for S4 increases after the torsion test.



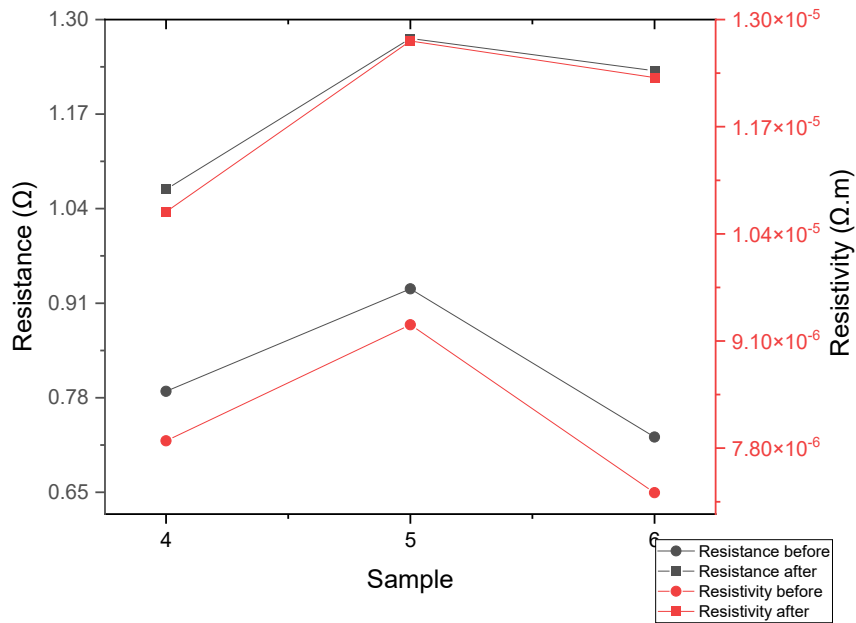
**Fig. 8.** Resistance and resistivity before and after torsion test on test samples for 3000 cycles

Table 5 shows the measured resistivity of the GNP hybrid before and after the 5000-cycle test. The average resistance and average resistivity for S4, S5, and S6 increase respectively after the torsion testing.

**Table 5**  
 Measurement of resistivity of the test samples for 5000 cycles of torsional testing

Sample	Average Resistance (Ω)		Average Resistivity (Ω.m)	
	before	after	before	after
S4	0.789	1.067	7.889e-06	1.067e-05
S5	0.930	1.274	9.296e-06	1.274e-05
S6	0.726	1.230	7.259e-06	1.230e-05
Average	0.815	1.190	8.148e-06	1.190e-05

Figure 9 illustrates the increment in the average resistivity value for all samples tested over 5000 cycles. The increase in resistance at 5000 cycles indicates the effect of low conductivity due to damage to the ink structure. According to [17], damage increases with distance from the beginning of twisting due to the fact that twisting strain increases with angle, distance from the axis of rotation, and starting length.



**Fig. 9.** Resistance and resistivity before and after torsion test on test samples for 5000 cycles

Table 6 displays resistivity measurements for all torsion cycles. The average resistance and resistivity for cycles 1000 and 3000 are lower than before testing. Meanwhile, after testing, the average resistivity of 5000 cycles increased. Each sample has a low standard deviation because graphene balances the pattern. The overall pattern of resistance remains fairly stable.

**Table 6**

Measurement of resistivity of the torsion test cycles

Cycle	Average Resistance (Ω)		Average Resistivity (Ω.m)		Standard deviation (Ω.m)
	before	after	before	after	
1000	1.073	0.816	1.073e-05	8.160e-06	7.423e-07
3000	0.816	0.815	8.160e-06	8.148e-06	5.805e-07
5000	0.815	1.190	8.148e-06	1.190e-05	6.597e-07

Figure 10 illustrates the pattern of the resistivity value before and after the torsion test for the particular cycles. The pattern is evident in the decrement of the resistivity value along with the increase in cycle numbers after the test. However, the 5000-cycle shows to be inversely increasing. Meanwhile, Figure 11 shows the average value of resistivity before and after torsional at all cycles. The results shown in Figure 10 have the biggest standard deviation for resistivity before cyclic torsion testing at 1000 cycles as compared to the others.

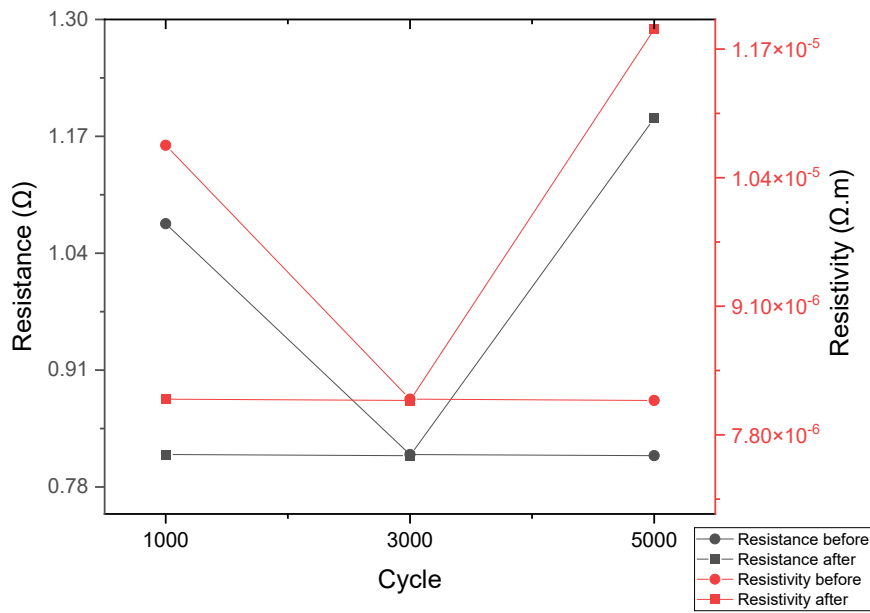


**Fig. 10.** Resistance and resistivity before and after torsion test on 1000, 3000, and 5000 cycles

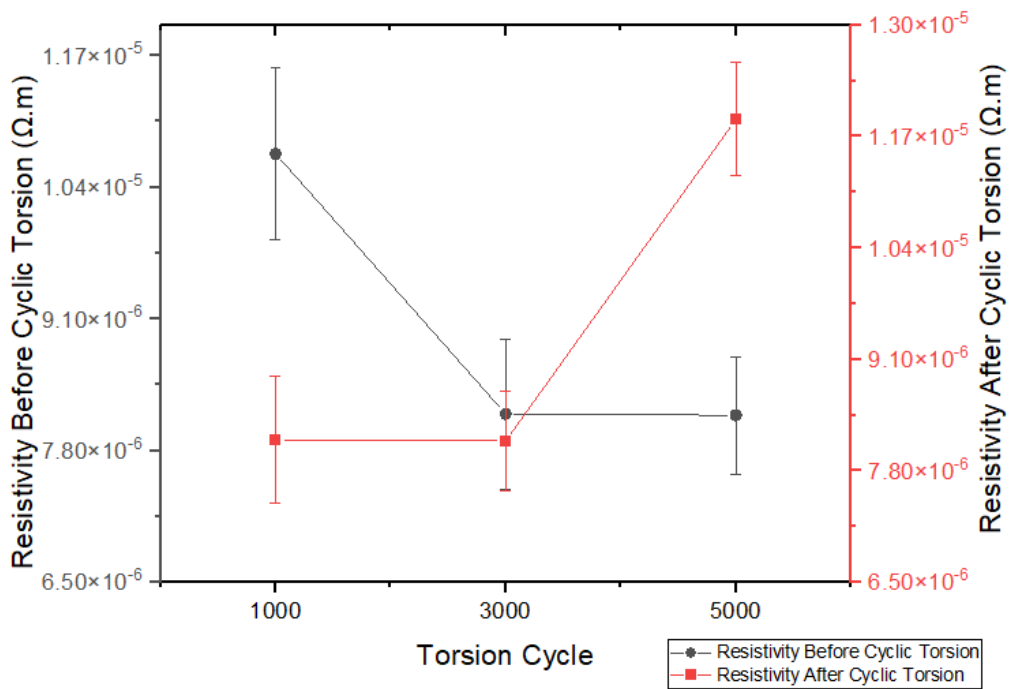


**Fig. 11.** Mean value of resistivity before and after cyclic torsion versus cycles

#### 4. Conclusions

The torsional experiments on GNP hybrid conductive ink were undertaken to validate the resistivity relationship of the new conductive ink formulation. The resistance values of samples S4, S5, and S6 decreased when exposed to torsion tests at 1000 and 3000 except at a cycle of 5000, when the resistance value rose, which is considered to be due to the damaging impact of increasing the number of torsion cycles on the sample. Extrusions and fractures caused by the irreversible motion

of dislocation in the metal interconnect increased the electrical resistance. In conclusion, the mechanical and torsional effects on stretchable GNP-Ag conductive ink have been investigated in several studies. The mechanical properties of the ink have been shown to be affected by mechanical stress and aging, while the electrical conductivity of the ink has been shown to be affected by torsional stress. These findings have important implications for the development of stretchable conductive inks for use in applications such as strain sensors and flexible electronics, as they highlight the need to carefully consider the mechanical and torsional properties of the ink in order to optimize their performance. In future work, it is recommended that the evaluation is made under temperature dependence and supported by SEM images.

### Acknowledgement

Thank you to Advanced Academia-Industry Collaboration Laboratory (AiCL) and Fakulti Kejuruteraan Mekanikal (FKM), Universiti Teknikal Malaysia Melaka (UTeM) for providing the laboratory facilities.

### References

- [1] Dang, Wenting, Vincenzo Vinciguerra, Leandro Lorenzelli, and Ravinder Dahiya. "Printable stretchable interconnects." *Flexible and Printed Electronics* 2, no. 1 (2017): 013003. <https://doi.org/10.1088/2058-8585/aa5ab2>
- [2] Chun, Sungwoo, Yeonhoi Choi, and Wanjun Park. "All-graphene strain sensor on soft substrate." *Carbon* 116 (2017): 753-759. <https://doi.org/10.1016/j.carbon.2017.02.058>
- [3] Choi, Suji, Sang Ihn Han, Dokyoon Kim, Taeghwan Hyeon, and Dae-Hyeong Kim. "High-performance stretchable conductive nanocomposites: materials, processes, and device applications." *Chemical Society Reviews* 48, no. 6 (2019): 1566-1595. <https://doi.org/10.1039/C8CS00706C>
- [4] Fiori, Gianluca, Francesco Bonaccorso, Giuseppe Iannaccone, Tomás Palacios, Daniel Neumaier, Alan Seabaugh, Sanjay K. Banerjee, and Luigi Colombo. "Electronics based on two-dimensional materials." *Nature nanotechnology* 9, no. 10 (2014): 768-779. <https://doi.org/10.1038/nnano.2014.207>
- [5] Khan, Junaid, Syed Abdul Momin, and M. Mariatti. "A review on advanced carbon-based thermal interface materials for electronic devices." *Carbon* 168 (2020): 65-112. <https://doi.org/10.1016/j.carbon.2020.06.012>
- [6] Dandu, Sridevi, Venkata Ramana Murthy Chitrapu, and Udaya Bhaskara Varma Nadimpalli. "Radiation Absorption and Diffusion Thermo Effects on Unsteady MHD Casson Fluid Flow Past a Moving Inclined Plate Embedded in Porous Medium in the Presence of Chemical Reaction and Thermal Radiation." *Journal of Advanced Research in Applied Sciences and Engineering Technology* 32, no. 3 (2023): 92-107. <https://doi.org/10.37934/araset.32.3.92107>
- [7] Shrivastava, Pankaj, Syed Nasimul Alam, Arka Ghosh, and Krishanu Biswas. "Fabrication, characterization, and mechanical properties and wear characteristics of graphite nanoplatelets incorporated nanotwinned Cu composites." *Diamond and Related Materials* 140 (2023): 110530. <https://doi.org/10.1016/j.diamond.2023.110530>
- [8] Htwe, Y. Z. N., and M. Mariatti. "Performance of water-based printed hybrid graphene/silver nanoparticle conductive inks for flexible strain sensor applications." *Synthetic Metals* 300 (2023): 117495. <https://doi.org/10.1016/j.synthmet.2023.117495>
- [9] Liu, Feixiang, Xinbin Qiu, Jianfeng Xu, Jianhua Huang, Danqing Chen, and Guohua Chen. "High conductivity and transparency of graphene-based conductive ink: Prepared from a multi-component synergistic stabilization method." *Progress in Organic Coatings* 133 (2019): 125-130. <https://doi.org/10.1016/j.porgcoat.2019.04.043>
- [10] Tran, Tuan Sang, Naba Kumar Dutta, and Namita Roy Choudhury. "Graphene inks for printed flexible electronics: Graphene dispersions, ink formulations, printing techniques and applications." *Advances in colloid and interface science* 261 (2018): 41-61. <https://doi.org/10.1016/j.cis.2018.09.003>
- [11] Htwe, Y. Z. N., and M. Mariatti. "Printed graphene and hybrid conductive inks for flexible, stretchable, and wearable electronics: Progress, opportunities, and challenges." *Journal of Science: Advanced Materials and Devices* 7, no. 2 (2022): 100435. <https://doi.org/10.1016/j.jsamd.2022.100435>
- [12] Sim, Sung-min, Yeonsu Lee, Hye-Lim Kang, Kwon-Yong Shin, Sang-Ho Lee, and Jung-Mu Kim. "RF performance of ink-jet printed microstrip lines on rigid and flexible substrates." *Microelectronic Engineering* 168 (2017): 82-88. <https://doi.org/10.1016/j.mee.2016.11.011>
- [13] Khan, Yasser, Mohit Garg, Qiong Gui, Mark Schadt, Abhinav Gaikwad, Donggeon Han, Natasha AD Yamamoto et al. "Flexible hybrid electronics: Direct interfacing of soft and hard electronics for wearable health

- monitoring." *Advanced Functional Materials* 26, no. 47 (2016): 8764-8775. <https://doi.org/10.1002/adfm.201603763>
- [14] Lall, Pradeep, Jinesh Narangaparambil, Ben Leever, and Scott Miller. "Flexure and twist test reliability assurance of flexible electronics." *Journal of Electronic Packaging* 142, no. 3 (2020): 031121.
- [15] Chow, Justin H., Jeffrey Meth, and Suresh K. Sitaraman. "Twist testing for flexible electronics." In *2019 IEEE 69th Electronic Components and Technology Conference (ECTC)*, pp. 785-791. IEEE, 2019.
- [16] Deng, Shaojia, Xin Zhang, Guowei David Xiao, Kai Zhang, Xiaowu He, Shihan Xin, Xinlu Liu, Anhui Zhong, and Yang Chai. "Thermal interface material with graphene enhanced sintered copper for high temperature power electronics." *Nanotechnology* 32, no. 31 (2021): 315710. <https://doi.org/10.1088/1361-6528/abfc71>
- [17] Mokhlis, M. "A Study On Mechanical and Electrical Properties of Hybridized Graphene-Carbon Nanotube Filled Conductive Ink." PhD diss., Master Dissertation, Universiti Teknikal Malaysia Melaka, 2020.
- [18] Yang, Jung-Kwon, Young-Joo Lee, Seol-Min Yi, Byoung-Joon Kim, and Young-Chang Joo. "Effect of twisting fatigue on the electrical reliability of a metal interconnect on a flexible substrate." *Journal of Materials Research* 33, no. 2 (2018): 138-148. <https://doi.org/10.1557/jmr.2017.422>